EAI Endorsed Transactions
on Digital Transformation of Industrial Processes Research Article **EAI.EU**

Selected Control Strategies for Nonlinear Technological Processes

E. Gavendová [1,*], J. Vojtěšek[1], F. Gazdoš[1]

[1] Faculty of Applied Informatics, Tomas Bata University in Zlin, nam. T. G. Masaryka 5555, CZ-760 01 Zlín, Czech Republic

Abstract

Nonlinear dynamics are frequently encountered in industrial processes, where conventional linear controllers often fail to ensure the required performance or safety due to phenomena such as multiple equilibria, limit cycles, and bifurcations, all of which can negatively impact system stability. These challenges necessitate control strategies that can adapt to changing operating conditions and capture nonlinear behavior more effectively. Building on earlier research, this study identifies and evaluates two promising approaches to model-based adaptive control suitable for nonlinear technological processes.

Within an established classification framework, two representative strategies are examined: one based on sequential linearization combined with polynomial control, and another employing a direct nonlinear method based on the Wiener model. Experimental validation is conducted on a two-tank benchmark and a continuous stirred-tank reactor, both representing typical nonlinear industrial systems.

The results show that sequential linearization in combination with polynomial control achieves faster set-point tracking, quicker convergence, and greater robustness compared to Wiener model control. These findings underscore the advantages of structured sequential linearization techniques within adaptive control and demonstrate their potential as a practical and effective alternative to purely linear control designs in complex nonlinear environments.

Keywords: Industrial Processes, Nonlinear Systems, Process Control, Nonlinear Control Methods.

Received on 22 October 2025, accepted on 21 November 2025, published on 26 November 2025

doi: 10.4108/dtip.10684

1. Introduction

A nonlinear dynamic system is a model suitable for describing a wide range of even very complex real-world phenomena across various industries. Its main disadvantage is the need to use more advanced and demanding mathematical framework, such as description by systems of nonlinear differential equations [1], [2] which very often prevents it from practical implementation. On the other hand, employing them may result in more precise and reliable control.

Although many state-of-the-art methods for nonlinear control exist, their applicability in practice is frequently restricted by assumptions such as the availability of accurate models, high computational requirements, or limited robustness to model uncertainties. These limitations highlight the need for approaches that balance theoretical rigor with practical implementability.

This work addresses these limitations by focusing on two control strategies that aim to reduce implementation complexity while maintaining satisfactory control performance. The first is control based on sequential linearization combined with a 1DOF control approach,

[*]Corresponding author. Email: egavendova@utb.cz

where DOF denotes the degree of freedom, and control employing the Wiener model. The goal is to evaluate how these approaches compare in terms of feasibility, accuracy, and computational demands.

Based on these aims, the paper addresses the following research question:

- How does the performance of Wiener-model-based control compare with sequential linearization with polynomial 1DOF approach when applied to the same system?

The paper is divided into two sections – theoretical and application-oriented. The theoretical section first introduces the representation of a nonlinear system and its typical phenomena, followed by a basic classification of control strategies and subsequently an overview of those used in nonlinear control. It then focuses on two selected approaches – control based on sequential linearization combined with a 1DOF control approach, and control employing the Wiener model. In the application section, the first approach is applied to a two-tank system in series, while the second is used for the control of a chemical reactor. For comparison purposes, both approaches are then applied to the two-tank system.

1.1 State-space description of a nonlinear system

Nonlinear dynamic systems are typically described in the time domain using nonlinear differential equations [1], [2] In many cases, the most suitable state-space representation for further steps is given by a system of ordinary nonlinear differential equations.

The continuous nonlinear dynamic system is generally described by the state equations:

$$\dot{\boldsymbol{x}}(t) = \boldsymbol{f}[t, \boldsymbol{x}(t), \boldsymbol{u}(t)], \quad (1)$$

and the output equation:

$$\boldsymbol{y}(t) = \boldsymbol{g}[t, \boldsymbol{x}(t), \boldsymbol{u}(t)] \quad (2)$$

Where $\dot{\boldsymbol{x}}(t)$ is the derivative of the system state vector $\boldsymbol{x} \in \mathbb{R}^n$, t represents time, $\boldsymbol{u} \in \mathbb{R}^m$ is the input vector and $\boldsymbol{y} \in \mathbb{R}^r$ is the output vector, $\boldsymbol{f} \in \mathbb{R}^n$ and $\boldsymbol{g} \in \mathbb{R}^r$ are generally nonlinear vector function [1], [2].

For a time-invariant system, where the vector functions $\boldsymbol{f}$ and $\boldsymbol{g}$ are not explicitly time-dependent, a simpler model can be obtained as follows:

$$\dot{\boldsymbol{x}}(t) = \boldsymbol{f}[\boldsymbol{x}(t), \boldsymbol{u}(t)] \quad (3)$$

$$\boldsymbol{y}(t) = \boldsymbol{g}[\boldsymbol{x}(t), \boldsymbol{u}(t)] \quad (4)$$

1.2 Typical phenomena of nonlinear systems

Certain phenomena are characteristic of nonlinear systems which do not occur in linear systems. Among the most significant of these phenomena are the existence of multiple or no solutions, finite-time escape, multiple isolated equilibria, limit cycles, synchronization, bifurcations, and other complex dynamic behaviours (such as chaos, turbulence, etc.) [1], [2].

2. Nonlinear control methods classification

There are two main groups of control methods for nonlinear systems:

A. Linearization of the system followed by the application of linear control methods.
B. Direct application of nonlinear control methods on the nonlinear system.

The choice of the appropriate approach depends on the system characteristics (such as the degree of nonlinearity and system complexity), whether the system remains in the vicinity of the operating point, and the required control precision [1], [2], [3].

When discussing the first group, a wide range of linearization methods can be applied, exhibiting negligible to zero deviation from the original nonlinear model, such as the Sequential Linearization [1], [2], [4] illustrated in Figure 1 or Exact Linearization [1], [2], [5] methods. The Exact Linearization method, described in detail in e.g. [2], [5] is computationally demanding and thus unsuitable for complex systems. The Sequential Linearization method is suitable for a broader range of systems. The core idea of the Sequential Linearization method is to create a linearized model at each point of the system's static characteristic, resulting in an accurate linearization of the nonlinear system [1], [2], [3].

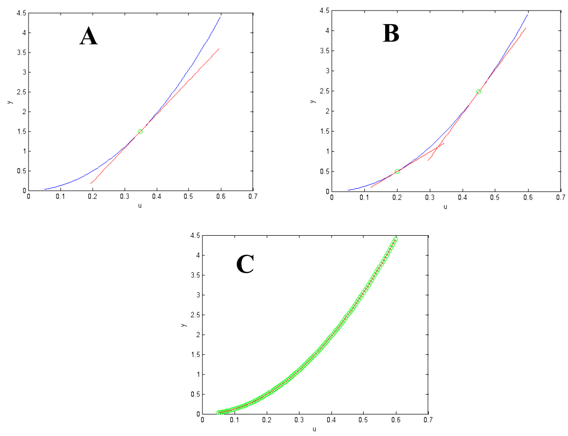

Figure 1. Comparison of linearization in 1 point (A), 2 points (B) and many points (C) used in Sequential Linearization.

A key advantage of this group is the availability of numerous linear control techniques applicable to the linearized model, ranging from basic controllers to advanced strategies, such as adaptive, robust, predictive control, and others.

The second mentioned group consists of methods directly applicable to nonlinear systems. A major limitation is the difficulty in identifying a suitable method, as many approaches are designed for specific systems with limited applicability to others. This group can be further divided into smaller subgroups, ordered chronologically based on their introduction:

1. Sliding Mode Control (SMC) [2] and its advanced variant, Integral SMC [6].
2. Adaptive control methods [2], [6], including Model Reference Adaptive Control (MRAC) [2], [6], Self-Tuning Adaptive Control (STAC) [6], Wiener/Hammerstein model-based control [1], [3], [4] and others.
3. Passivity-Based Control (PBC) [6].
4. Model Predictive Control (MPC) [6] and its nonlinear extension, Nonlinear MPC (NMPC) [7].
5. Optimal Control [8] and Nonlinear Programming [9].
6. Neural Network [10] and Artificial Intelligence-based approaches [11] - Reinforcement Learning [12], Fuzzy Logic [2], etc.
7. Data-driven control methods, e.g. [3], [13].

2.1. Selected model-based control methods

An overview of selected model-based methods for nonlinear systems control is provided in [1], [2], [3]. The last-mentioned compares control results for two-tank nonlinear system from both group A and B. From group A, the method of sequential linearization followed by polynomial control using a 1DOF configuration was selected, while from group B, control with a Wiener model was chosen. For further testing the methods mentioned above, three reference values of the output were required. The method of sequential linearization with polynomial control design reached the desired values more quickly and achieved significantly better results in this comparison.

3. Control via Sequential Linearization

Since the sequential linearization method also provides an input–output description of the system, linear control design methods requiring such a representation can be easily employed.

The polynomial control approach [3], [14], [15] is based on transfer functions of individual elements of a control loop, which are treated as ratios of polynomials. The controller structure and its parameter values are obtained by solving polynomial equations. This synthesis approach is suitable for a wide range of systems — those with non-minimum phase behaviour, integrative properties, unstable dynamics, and for various types of reference and disturbance signals [4], [14], [15].

The polynomial synthesis method can be generally used for different control system configurations, most commonly 1DOF and 2DOF structures [4], [14]. For subsequent control based on sequential linearization, the 1DOF configuration was selected, representing a classical feedback controller connection as presented below, in Figure 2.

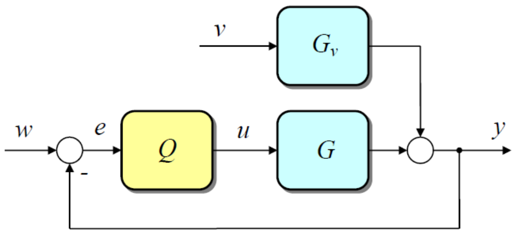

Figure 2. 1DOF control configuration scheme

The blocks G and G_v represent the transfer functions of the control and disturbance channels of the plant, respectively, while Q denotes the feedback controller. Transfer functions of these elements are generally described by (5). The signal y is the controlled variable, u is the control input, v is the disturbance, e is the control error, and w is the reference signal. Laplace transforms of these signals are denoted by uppercase letters with s denoting complex variable of the Laplace transform. These transforms are further substituted by polynomials: $a(s)$ as the denominator of the control and disturbance channels of the plant, $b(s)$ and $c(s)$ as their numerators, and $p(s)$ as the denominator of the regulator and $q(s)$ as its numerator.

$$\begin{aligned} G(s) &= \frac{Y(s)}{U(s)} = \frac{b(s)}{a(s)} \\ G_v(s) &= \frac{Y(s)}{V(s)} = \frac{c(s)}{a(s)} \\ Q(s) &= \frac{U(s)}{E(s)} = \frac{q(s)}{p(s)} \end{aligned} \tag{5}$$

Generally, the reference and disturbance inputs can also be expressed as ratios of polynomials,

$$W(s) = \frac{h_w(s)}{f_w(s)}, \qquad V(s) = \frac{h_v(s)}{f_v(s)} \tag{6}$$

The polynomial equation whose solution provides the controller parameters and defines the degrees of polynomials in the polynomial equation arises from the following control objectives:

a) stability of the closed loop system,
b) inner properness (physical realizability of all the elements),
c) asymptotic tracking of the reference signal,
d) full disturbance rejection,

e) required control performance (given by the pole assignment problem solution).

For the basic requirements above, which may be further extended, the following polynomial equation can be derived:

$$a(s)f(s)\tilde{p}(s) + b(s)q(s) = d(s), \quad p(s) = f(s)\tilde{p}(s) \qquad (7)$$

where $f(s)$ is the least common multiple of the polynomials $f_w(s)$ and $f_v(s)$, defined by the shapes of the input signals of the reference and disturbance. The unknown polynomials are $\tilde{p}(s)$ and $q(s)$, determining the controller transfer function and closed-loop characteristic polynomial $d(s)$ defining the behavior of the resultant closed-loop. It can be derived that their degrees must satisfy

$$\begin{aligned} \deg q(s) &= \deg a(s) + \deg f(s) - 1 \\ \deg \tilde{p}(s) &\geq \deg a(s) - 1 \\ \deg d(s) &\geq 2\deg a(s) + \deg f(s) - 1 \end{aligned} \qquad (8)$$

The polynomial equation may be solved, for example, using the method of undetermined coefficients [1], [4], [14].

Selecting the polynomial $d(s)$ is the result of the so-called pole-assignment problem. To satisfy the stability condition, the characteristic polynomial $d(s)$ must be stable. Proper placement of the closed-loop poles affects not only stability but also the required control quality [4], [14], [15]. The general form of the polynomial can be written as

$$d(s) = \prod_{i=1}^{\deg d(s)} (s - s_i), \qquad (9)$$

Where s_i are, in general, complex numbers $s_i = \alpha_i + j\beta_i$, representing the characteristic polynomial poles. If the poles lie in the left-hand half-plane, i.e. $\alpha_i < 0$, the polynomial is stable. Real poles result in an aperiodic control response, whereas the presence of at least one complex-conjugate pair leads to an oscillatory response. The simplest case, how to choose this polynomial, is to define it with a single multiple pole, i.e. in the following form:

$$d(s) = (s + \alpha)^{\deg d(s)} \qquad (10)$$

Using this form may be inappropriate for some systems that are more difficult to control. However, it has the benefits of simple tuning of the resultant closed-loop behavior by one parameter $\alpha > 0$. Some recommended forms of $d(s)$ for stable aperiodic systems are presented below in (11), and for unstable non-oscillatory systems in (12),

$$d(s) = a(s)(s + \alpha)^{\deg d(s) - \deg a(s)} \qquad (11)$$

$$d(s) = n(s)(s + \alpha)^{\deg d(s) - \deg a(s)} \qquad (12)$$

where the polynomial $n(s)$ is obtained by spectral factorization from the polynomial equation

$$a^*(s)a(s) = n^*(s)n(s) \qquad (13)$$

where the asterisk * denotes complex-conjugate polynomial, i.e. $x^*(s) = x(-s)$. The polynomial control approach in the 2DOF control configuration will be used later as part of nonlinear control with a Wiener model.

4. Nonlinear Control of Nonlinear Systems

The term nonlinear control of nonlinear systems refers to methods that are not based on linearization of the system and subsequent controller design for a linearized model. These methods are therefore suitable also for higher-order systems with complex structures, where obtaining a sufficiently accurate linearized model becomes computationally infeasible [1], [2], [15].

Good results are achieved by approaches based on factorization of the system into a static nonlinear part and a dynamic linear part, known as Hammerstein and Wiener models [1], [2], [4], graphically presented in Figures 3 and 4.

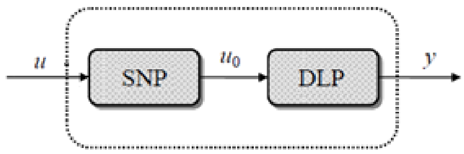

Figure 3. Hammerstein model of the system

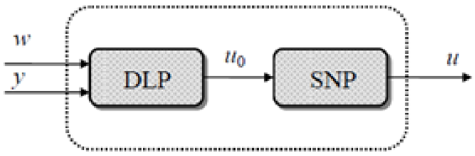

Figure 4. Wiener model of the system

The static nonlinear part usually evaluates the static characteristic based on the current value of the controlled variable [1], while the dynamic linear part is realized by linear control methods, e.g., a conventional PID controller, or e.g. the polynomial control approach in 1DOF or 2DOF control configuration used in this study [4].

4.1. Control with a Wiener Model

The following chapter introduces a specific approach to nonlinear control using the Wiener model, which will be applied in the practical part of this work to control a chemical reactor system and a series-connected liquid-tank system. As noted above, the Wiener model is based on decomposing the system into two parts. Consequently, the controller comprises two blocks: a static nonlinear part (SNP) and a dynamic linear part (DLP). A detailed scheme depicting both blocks with the input and output signals is shown in Figure 4 above, where *w*, *y*, and *u* correspond to conventional notation in control systems as presented in Figure 2. The signal u_0 is the output of the DLP and represents the deviation of the controlled variable with respect to its desired value [1], [4].

Static Nonlinear Part

The SNP is derived from a simulated or measured static characteristic that describes the dependence of the steady-state output $\eta(t)$ on the steady-state input $\upsilon(t)$. A working point υ^s, η^s, operating interval $\upsilon_{min} \leq \upsilon(t) \leq \upsilon_{max}$, and boundary values υ_L, υ_U satisfying $\upsilon_L \leq \upsilon^s \leq \upsilon_U$ must be selected by a designer. Then, according to the characteristic, the corresponding values are η_{min}, η_{max} and η_L, η_U. For control purposes we define

$$u(t) = \upsilon(t) - \upsilon^s, \qquad y(t) = \eta(t) - \eta^s \quad (14)$$

Then, using the auxiliary variables defined as

$$\gamma = \frac{\upsilon^s - \upsilon_L}{\upsilon_L}, \qquad \psi = \eta^s - \eta_L \quad (15)$$

a specific relationship $\psi = f(\gamma)$ is obtained [4], [14], [15].

In the next step we invert this relationship to obtain $\gamma = f(\psi)$, approximating it using a suitable polynomial, exponential, or other function [4], [15]. The change of the control input is then finally computed as

$$u(t) = \Delta\upsilon(t) = \upsilon_L \left(\frac{\mathrm{d}\gamma}{\mathrm{d}\psi}\right)_{\psi(\eta)} u_0(t) \quad (16)$$

External Linear Model

The system consisting of the SNP and plant model is continuously identified as a continuous-time external linear model (CT ELM) [4], [14]. Its general structure is determined from simulated step responses of this combined system, with adaptive approach allowing higher-order systems to be approximated by lower-order models with time-varying parameters. In general, the CT ELM can be written either as a differential equation

$$\sum_{i=0}^{n} a_i y^{(i)}(t) = \sum_{j=0}^{m} b_j u^{(j)}(t) \quad (17)$$

or transfer function

$$G(s) = \frac{Y(s)}{U_0(s)} = \frac{b(s)}{a(s)} = \frac{b_m s^m + \dots + b_1 s + b_0}{a_n s^n + \dots + a_1 s + a_0} \quad (18)$$

where a_i, b_j represent coefficients that are to be identified and updated adaptively.

Parameter Estimation

A direct estimation method is used for identifying the CT ELM parameters. Since the derivatives of the input and output signals cannot be measured directly, filtered variables u_{0f} and y_f are introduced, where the filter time constant must be generally smaller than that of the controlled process. The filters are then described by

$$c(\sigma)u_{0f}(t) = u_0(t), \quad (19)$$

$$c(\sigma)y_f(t) = y(t), \quad (20)$$

Where $\sigma = \mathrm{d}/\mathrm{d}t$ and $c(\sigma)$ is a stable polynomial satisfying $\deg c(\sigma) \geq \deg a(\sigma)$. Polynomials $a(\sigma)$ and $c(\sigma)$ are of the type $a(\sigma) = \sigma^n + a_{n-1}\sigma^{n-1} + \dots + a_1\sigma + a_0$ and their degree n is the same as the degree of CT ELM [4], [14].

Applying the Laplace transform gives

$$c(s)U_{0f}(s) = U_0(s) + \mu_1(s), \quad (21)$$

$$c(s)Y_f(s) = Y(s) + \mu_2(s), \quad (22)$$

with $\mu_1(s)$, $\mu_2(s)$ denoting initial condition terms.

Then substituting into (18) yields

$$\begin{aligned} Y_f(s) &= \frac{b(s)}{a(s)} U_{0f}(s) + M(s) \\ &= G(s)U_{0f}(s) + M(s), \end{aligned} \quad (23)$$

where $M(s)$ reflects the effect of initial conditions [4], [15]. The filtered variables and their derivatives are then sampled at times $t_k = kT_S$, $k = 0,1,2,\dots,$ where T_S is a sampling period.

The vector of estimated model parameters, denoted as

$$\mathbf{\Theta}^T(t_k) = [a_0 a_1 \dots a_{n-1} b_0 b_1 \dots b_m] \quad (24)$$

is computed from the following equation:

$$y_f^{(n)}(t_k) = \mathbf{\Theta}^T(t_k)\boldsymbol{\phi}(t_k) + \mu(t_k), \quad (25)$$

where $\boldsymbol{\phi}(t_k)$ denotes the regression vector and is defined as

$$\begin{aligned} \boldsymbol{\phi}(t_k) &= \\ &= \Big[-y_f(t_k) - y_f^{(1)}(t_k) \dots \\ &- y_f^{(n-1)}(t_k)\, u_{0f}(t_k)\, u_{0f}^{(1)}(t_k) \dots u_{0f}^{(m)}(t_k)\; 1\Big] \end{aligned} \quad (26)$$

Dynamic Linear Part

The linear part is then designed using the polynomial approach in a 2DOF control configuration comprising both, a feedback controller Q and a feedforward controller R, as shown in Figure 5 below.

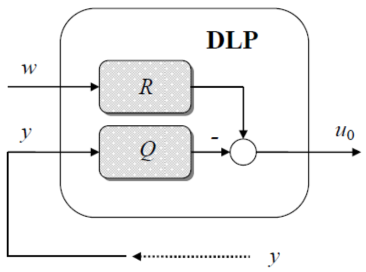

Figure 5. DLP in 2DOF configuration [1]

Here, signals w and y denote the reference and controlled variable respectively, while u_0 serves as the input to the CT ELM and SNP blocks. Disturbance v and reference w are assumed to be step functions with Laplace transforms

$$W(s) = \frac{w_0}{s}, V(s) = \frac{v_0}{s} \quad (27)$$

for some real values w_0, v_0. The controller transfer functions are generally assumed as

$$R(s) = \frac{r(s)}{p(s)}, Q(s) = \frac{q(s)}{p(s)} \quad (28)$$

with the properness condition for the controllers satisfied if

$$\deg r \leq \deg p, \deg q \leq \deg p \quad (29)$$

Considering step reference and disturbance inputs, then the polynomial $p(s)$ can be derived and re-written as

$$p(s) = s\tilde{p}(s) \quad (30)$$

The following control design requirements are imposed:

a) stability of the control loop,
b) physical realizability,
c) asymptotic tracking of the reference signal,
d) full disturbance rejection,
e) required closed-loop dynamics (given by the pole assignment problem solution).

Satisfying these requirements leads to the derivation of the following polynomial equations

$$\begin{aligned} a(s)s\tilde{p}(s) + b(s)q(s) &= d(s), \\ t(s)s + b(s)r(s) &= d(s) \end{aligned} \quad (31)$$

whose solution finally gives the controller parameters for a defined characteristic polynomial of the loop $d(s)$. Then, the degrees of the unknown polynomials can be derived as:

$$\begin{aligned} \deg q(s) &= \deg a(s) + \deg f_v(s) - 1 \\ \deg \tilde{p}(s) &= \deg a(s) - 1 + k \\ \deg d(s) &= 2\deg a(s) + \deg f_v(s) - 1 + k \\ \deg r(s) &= \deg f_w(s) - 1 \\ \deg t(s) &= 2\deg a(s) + \deg f_v(s) - \\ &\quad \deg f_w(s) - 1 + k \\ k &= \deg f_w(s) - \deg f_v(s) - \deg a(s) \end{aligned} \quad (32)$$

The constant k can only be zero or positive.

The characteristic polynomial $d(s)$ is chosen in this specific form:

$$d(s) = a(s)(s+\alpha)^{\deg d(s) - \deg a(s)} \quad (33)$$

which ensures good performance for aperiodic processes [4], [14] and further simple tuning by the one free parameter $\alpha > 0$. Then the polynomial equations (31) are solved via the method of undetermined coefficients, resulting in a matrix equation that yields the unknown controller parameters at each sampling instant [4], [14].

5. Applications

5.1. Linear Control of the System

In this section, the linear control methods introduced in the theoretical part above are demonstrated on selected system models of common industrial processes. For each method, a linearized model is computed, control design calculations are carried out based on this model, and finally a simulation validation of the control response is presented.

Liquid-Tank System in Series

A suitable nonlinear model for applying and testing linear control methods is e.g. a system of two cylindrical liquid tanks in series, which can be considered in both single-input single-output (SISO) and multi-input multi-output variants and is a common part of many industrial applications [1].

SISO Liquid-Tank System

The SISO system of cylindrical liquid tanks in series is shown in Figure 6 below.

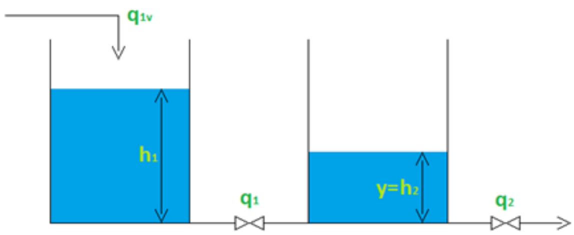

Figure 6. Scheme of the SISO cylindrical-tank system in series

The system input is the inflow to the first tank q_{1v}, the (controlled) output is the liquid level in the second tank h_2, and the states are the levels of liquid h_1 and h_2 in both the tanks. Output flows from the tanks are denoted by q_1 and q_2; the surface areas are represented by the constants F_1, F_2, and k_1, k_2 denote valve coefficients.

The simplified state-space description derived by the balance of the flows is given as

$$\begin{aligned} F_1 \frac{dh_1(t)}{dt} + q_1 &= q_{1v}, \\ F_2 \frac{dh_2(t)}{dt} + q_2 &= q_1, \end{aligned} \quad (34)$$

where the output flows can be modelled as:

$$q_1 = k_1\sqrt{|h_1 - h_2|}, q_2 = k_2\sqrt{h_2} \quad (35)$$

Substitution yields

$$\frac{dh_1(t)}{dt} = \frac{q_{1v}}{F_1} - \frac{k_1}{F_1}\sqrt{|h_1 - h_2|}, \quad (36)$$

$$\frac{\mathrm{d}h_2(t)}{\mathrm{d}t} = \frac{k_1}{F_2}\sqrt{|h_1 - h_2|} - \frac{k_2}{F_2}\sqrt{h_2}$$

Steady-state values are obtained by setting the derivatives in the state equations above equal to zero, resulting in the nonlinear equations:

$$q_{1v}^s = k_1\sqrt{|h_1^s - h_2^s|},\ q_{2v}^s = k_2\sqrt{|h_2^s|} \quad (37)$$

For simulation purposes and subsequent control design purposes, a Simulink subsystem *SISO_tank_system* was created as presented in Figure 7 below.

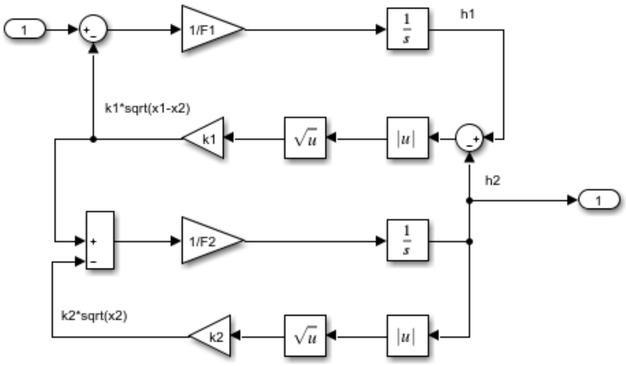

Figure 7. Simulink model of SISO tanks in series

Control of the Liquid-Tank System Using Sequential Linearization

The sequential linearization control method [1] was applied to the SISO liquid-tank system. The core idea of the method is to compute an approximate linearization at the point on the static characteristic where the system is currently operating. Therefore, the actual tank levels are required as input information so that a linearized model is computed at each step.

Initial conditions are generally given as

$$h_1(0) = h_{10},\ h_2(0) = h_{20} \quad (38)$$

Considering system description (34), (35), the linearization in a general operating point h_{1i}, h_{2i} yields

$$\begin{aligned} \Delta q_1 &= \left(\frac{\partial q_1}{\partial h_1}\right)_{h_{1i},h_{2i}} \Delta h_1 + \left(\frac{\partial q_1}{\partial h_2}\right)_{h_{1i},h_{2i}} \\ \Delta h_2 &= \frac{k_1}{2\sqrt{h_{1i} - h_{2i}}}(\Delta h_1 - \Delta h_2) \\ \Delta h_2 &= \frac{k_1\sqrt{h_{1i} - h_{2i}}}{2(h_{1i} - h_{2i})}(\Delta h_1 - \Delta h_2) = K_{1i}(\Delta h_1 - \Delta h_2) \end{aligned} \quad (39)$$

$$\begin{aligned} \Delta q_2 = \left(\frac{\partial q_2}{\partial h_2}\right)_{h_{1i},h_{2i}} \Delta h_2 = \frac{k_2}{2\sqrt{h_{2i}}}\Delta h_2 = \frac{k_2\sqrt{h_{2i}}}{2h_{2i}}\Delta h_2 \\ = K_{2i}\Delta h_2 \end{aligned} \quad (40)$$

where by substituting the deviation variables as $\Delta h_1 = x_1$, $\Delta h_2 = x_2$, $\Delta q_{1v} = u_1$, the linearized model is described as

$$\begin{aligned} \dot{x}_1 &= a_{11,i}x_1 + a_{12,i}x_2 + bu_1 \\ \dot{x}_2 &= a_{21,i}x_1 + a_{22,i}x_2 \\ y &= x_2 \end{aligned} \quad (41)$$

with

$$\begin{aligned} a_{11,i} = -\frac{K_{1i}}{F_1}, a_{12,i} = \frac{K_{1i}}{F_1}, \\ a_{21,i} = \frac{K_{1i}}{F_2}, a_{22,i} = -\frac{K_{1i} + K_{2i}}{F_2}, b = \frac{1}{F_1} \end{aligned} \quad (42)$$

where K_{1i}, K_{2i} are defined as:

$$\begin{aligned} K_{1i} &= \frac{k_1\sqrt{h_{1i} - h_{2i}}}{2(h_{1i} - h_{2i})} \\ K_{2i} &= \frac{k_2\sqrt{h_{2i}}}{2h_{2i}} \end{aligned} \quad (43)$$

The state-space form of the linearized model then reads:

$$\begin{aligned} \dot{\boldsymbol{x}}(t) &= \boldsymbol{A}_i\boldsymbol{x}(t) + \boldsymbol{B}u(t) \\ y(t) &= \boldsymbol{C}\boldsymbol{x}(t) \end{aligned} \quad (43)$$

with

$$\boldsymbol{A}_i = \begin{pmatrix} a_{11,i} & a_{12,i} \\ a_{21,i} & a_{22,i} \end{pmatrix}, \boldsymbol{B} = \begin{pmatrix} b \\ 0 \end{pmatrix}, \boldsymbol{C} = \begin{pmatrix} 0 & 1 \end{pmatrix}\frac{1}{F_1} \quad (44)$$

The transfer function of this system is then computed as

$$\begin{aligned} \boldsymbol{G}(s) &= \boldsymbol{C}(s\boldsymbol{I} - \boldsymbol{A}_i)^{-1}\boldsymbol{B} \\ &= \frac{1}{\det(s\boldsymbol{I} - \boldsymbol{A}_i)}\boldsymbol{C}\mathrm{adj}(s\boldsymbol{I} - \boldsymbol{A}_i)\boldsymbol{B} \\ &= \frac{b(s)}{a(s)} = \frac{b_{0,i}}{s^2 + a_{1,i}s + a_{0,i}} \end{aligned} \quad (45)$$

with

$$\begin{aligned} b_{0,i} = ba_{21,i}, a_{1,i} = -a_{11,i} - a_{22,i}, \\ a_{0,i} = a_{11,i}a_{22,i} - a_{12,i}a_{21,i} \end{aligned} \quad (46)$$

Control of the SISO Tanks in Series Using the Polynomial Approach with 1DOF Configuration

The controller is designed for each linearized model using the polynomial approach outlined earlier in this paper in the 1DOF structure [4], [14], [15]. The transfer functions in (5), (6) take for this plant the specific form

$$\begin{aligned} G(s) &= \frac{Y(s)}{U(s)} = \frac{b(s)}{a(s)} = \frac{b_{0,i}}{s^2 + a_{1,i}s + a_{0,i}} \\ Q(s) &= \frac{U(s)}{E(s)} = \frac{q(s)}{p(s)} = \frac{q_{2,i}s^2 + q_{1,i}s + q_{0,i}}{s(s + \tilde{p}_{0,i})} \end{aligned} \quad (47)$$

Both reference and disturbance signals are generally considered as step signals for some real values w_0, v_0,

$$W(s) = \frac{w_0}{s}, \qquad V(s) = \frac{v_0}{s} \quad (48)$$

Controller parameters are obtained from the polynomial equation (7), where *f(s)=s*, using the method of undetermined coefficients. The characteristic polynomial *d(s)* has the form (33) and the polynomial degrees must satisfy (8), hence:

$$(s^2 + a_{1,i}s + a_{0,i})s(s + \tilde{p}_{0,i}) + b_{0,i}(q_{2,i}s^2 + q_{1,i}s + q_{0,i}) = n(s)(s+\alpha)^2, \tag{49}$$

where $\alpha > 0$ is an optional tuning parameter that can be used to further tune the achieved control responses. For the coefficients of the polynomial $n(s)$, the following relations can be derived (see eq. 12 and 13):

$$n(s) = s^2 + n_{1,i}s + n_{0,i}, n_{0,i} = \sqrt{a_{0,i}^2}, n_{1,i} = \sqrt{a_{1,i}^2 + 2n_{0,i} - 2a_{0,i}} \tag{50}$$

The method of undetermined coefficients finally yields this matrix equation for the unknown controller parameters

$$\begin{pmatrix} \tilde{p}_{0,i} \\ q_{2,i} \\ q_{1,i} \\ q_{0,i} \end{pmatrix} = \begin{pmatrix} 1 & 0 & 0 & 0 \\ a_{1,i} & b_{0,i} & 0 & 0 \\ a_{0,i} & 0 & b_{0,i} & 0 \\ 0 & 0 & 0 & b_{0,i} \end{pmatrix}^{-1} \begin{pmatrix} d_{3,i} - a_{1,i} \\ d_{2,i} - a_{0,i} \\ d_{1,i} \\ d_{0,i} \end{pmatrix} \tag{51}$$

with

$$d_{3,i} = n_{1,i} + 2\alpha, d_{2,i} = 2\alpha n_{1,i} + n_{0,i} + \alpha^2, d_{1,i} = 2\alpha n_{0,i} + \alpha^2 n_{1,i}, d_{0,i} = \alpha^2 n_{0,i} \tag{52}$$

Initial Controller Settings

To perform control, an initial setting of the controller parameters must be chosen. This is obtained from a control simulation based on linearization in a single operating point. The simulation results and testing also provide a suitable value of the tuning parameter α. The simulation experiments were performed using the following constant values:

$$F_1 = 2\ m^2 \quad k_1 = 0.283\ m^{2.5}/min \quad q_{1v}^s = 0.2\ m^3/min$$
$$F_2 = 1.8\ m^2 \quad k_2 = 0.286\ m^{2.5}/min \quad q_{2v}^s = 0.15\ m^3/min$$

Controller parameters were computed only once at the beginning of the simulation using the above given relations. For various α values, simulation results are shown in Figure 9 (see the simulation scheme in Figure 8).

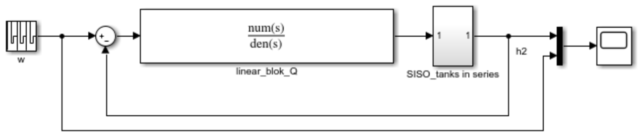

Figure 8. Simulation scheme used in the adaptation phase

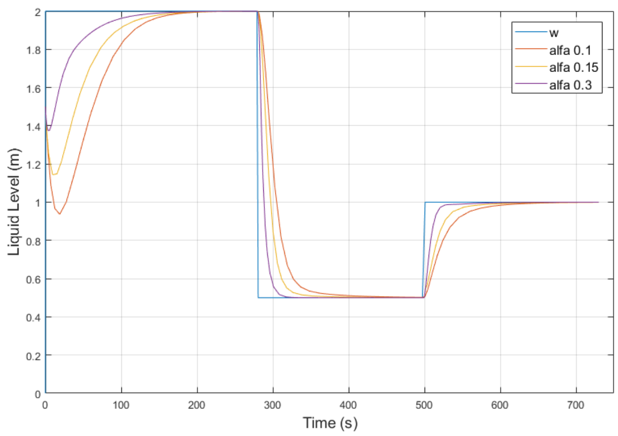

Figure 9. Level responses in the second tank for different values of *α*

Figure 9 shows that the good results are obtained for α = 0.3 where smaller under-shoot and faster response is achieved. The simulation testing also revealed that for smaller values of α, the control quality decreases, while for larger values the closed-loop system becomes unstable. Based on this information, the initial controller parameters were therefore calculated as follows:

$$\tilde{p}_0 = 0.6000 \quad q_2 = 1.6191 \quad q_1 = 0.4470 \quad q_0 = 0.0105$$

Simulation of Sequential Linearization Control

The simulation uses the same constants and initial controller settings obtained above. At each simulation step, a linearized model is computed from the current output and the controller Q is updated accordingly using the formulas (28). The implementation in the MATLAB/Simulink is presented in Figure 10 below followed by some simulation results in Figure 11.

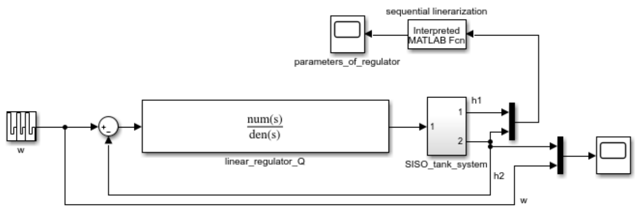

Figure 10. Simulation scheme of the sequential linearization control

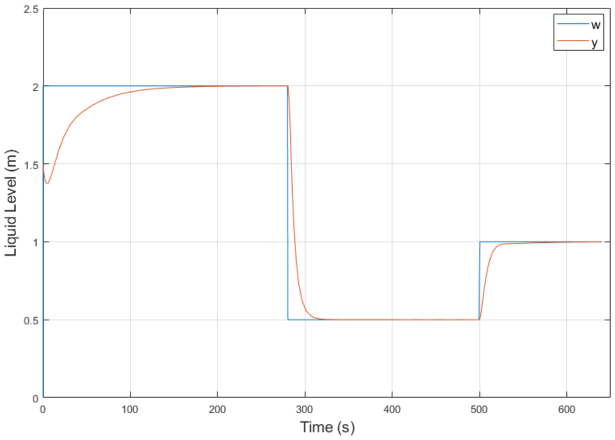

Figure 11. Closed-loop response under the sequential linearization method

The obtained results demonstrate that the proposed control method effectively fulfils its purpose – it provides stable control process with asymptotic tracking of the reference signal and consequently it can be considered successful for this class of systems.

5.2. Nonlinear Control of the System

Nonlinear control refers to methods used for controlling nonlinear systems that do not require a linearized model. In this work, control approach based on the Wiener model is employed, which is suitable for a broad range of nonlinear systems. A major advantage of the method is its applicability to higher-order systems with complex structure [4], [14] which are frequently present in many industrial applications. Therefore, the method is demonstrated further on the control of a continuous stirred tank reactor (CSTR) [4], [14] which is a common part of many production processes.

Control of a Continuous Stirred Tank Reactor

A CSTR with an exothermic first-order reaction of the form $A \xrightarrow{k_1} B \xrightarrow{k_2} C$ with a perfectly mixed cooling jacket is considered here. The system can be then described by the mathematical model in the form of four ordinary differential equations [4] where the first two are derived from the material balances and the remaining two come from heat balances inside the reactor:

$$\frac{\mathrm{d}c_{\mathrm{A}}}{dt} = -\left(\frac{q_{\mathrm{r}}}{V_{\mathrm{r}}} + k_1\right) c_{\mathrm{A}} + \frac{q_{\mathrm{r}}}{V_{\mathrm{r}}} c_{\mathrm{Af}} \qquad (53)$$

$$\frac{\mathrm{d}c_{\mathrm{B}}}{dt} = -\left(\frac{q_{\mathrm{r}}}{V_{\mathrm{r}}} + k_2\right) c_{\mathrm{B}} + k_1 c_{\mathrm{A}} + \frac{q_{\mathrm{r}}}{V_{\mathrm{r}}} c_{\mathrm{Bf}} \qquad (54)$$

$$\frac{\mathrm{d}T_{\mathrm{r}}}{dt} = \frac{h_{\mathrm{r}}}{\left(\rho c_p\right)_{\mathrm{r}}} + \frac{q_{\mathrm{r}}}{V_{\mathrm{r}}}(T_{\mathrm{rf}} - T_{\mathrm{r}}) + \frac{A_{\mathrm{h}} U}{V_{\mathrm{r}}\left(\rho c_p\right)_{\mathrm{r}}}(T_{\mathrm{c}} - T_{\mathrm{r}}) \qquad (55)$$

$$\frac{\mathrm{d}T_{\mathrm{c}}}{dt} = \frac{q_{\mathrm{c}}}{V_{\mathrm{c}}}(T_{\mathrm{cf}} - T_{\mathrm{c}}) + \frac{A_{\mathrm{h}} U}{V_{\mathrm{c}}\left(\rho c_p\right)_{\mathrm{c}}}(T_{\mathrm{r}} - T_{\mathrm{c}}) \qquad (56)$$

with initial conditions defined as

$$c_{\mathrm{A}}(0) = c_{\mathrm{A}}^{\mathrm{s}}, c_{\mathrm{B}}(0) = c_{\mathrm{B}}^{\mathrm{s}}, T_{\mathrm{r}}(0) = T_{\mathrm{r}}^{\mathrm{s}}, \quad T_{\mathrm{c}}(0) = T_{\mathrm{c}}^{\mathrm{s}} \qquad (57)$$

Here c denotes concentrations, T temperatures, V volumes, ρ densities, c_p specific heat capacities, q volumetric flow rates, A_h heat-transfer area, and U the heat-transfer coefficient. The subscript $(\cdot)_r$ refers to reactor variables, $(\cdot)_c$ to cooling variables, $(\cdot)_f$ to steady-state inputs and $(\cdot)_s$ to initial conditions. The kinetic rate constants and reaction heat are described as

$$k_j = k_{0j} \exp\left(\frac{-E_j}{R T_{\mathrm{r}}}\right), j = 1, 2 \qquad (58)$$

$$h_{\mathrm{r}} = h_1 k_1 c_{\mathrm{A}} + h_2 k_2 c_{\mathrm{B}} \qquad (59)$$

A Simulink subsystem *CSTR* presented in Figure 12 was created for analysis of the model and control system design purposes.

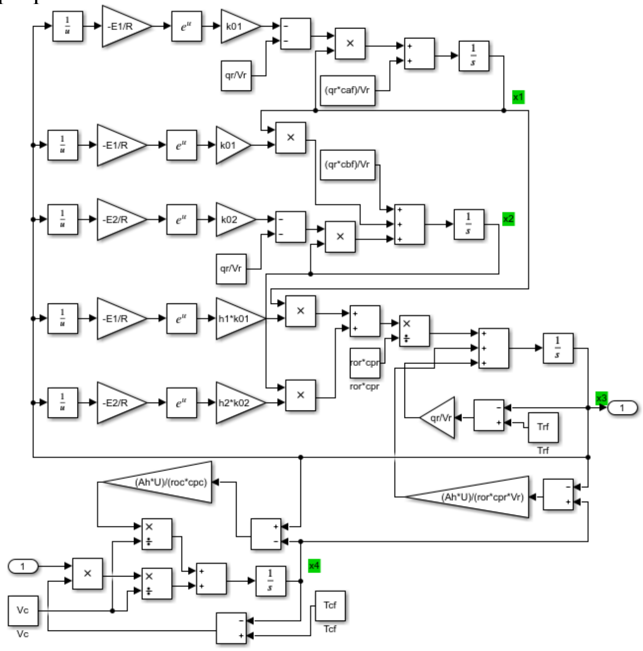

Figure 12. Simulink model of the CSTR system

For the simulation experiments, the parameters and steady-state conditions are listed in Table 1.

Table 1. Parameters, steady-state inputs and initial conditions of CSTR model.

$V_r = 1.2\, m^3$	$c_{pr} = 4.05\, kJ\, kg^{-1}K^{-1}$
$T_r^s = 324.80\, K$	$V_c = 0.64\, m^3$
$c_{pc} = 4.18\, kJ\, kg^{-1}K^{-1}$	$T_c^s = 306.28\, K$
$\rho_r = 985\, kg\, m^{-3}$	$A_h = 5.5\, m^2$
$c_{Af}^s = 2.85\, kmol\, m^{-3}$	$\rho_c = 998\, kg\, m^{-3}$
$U = 43.5\, kJ\, m^{-2}min^{-1}K^{-1}$	$c_{Bf}^s = 0\, kmol\, m^{-3}$
$k_{10} = 5.616 \cdot 10^{16}\, min^{-1}$	$E_1/R = 13477\, K$
$T_{rf}^s = 323\, K$	$k_{20} = 1.128 \cdot 10^{18}\, min^{-1}$
$E_2/R = 15290\, K$	$T_{cf}^s = 293\, K$
$h_1 = 4.8 \cdot 10^4\, kJ\, kmol^{-1}$	$c_A^s = 1.5796\, kmol\, m^{-3}$
$q_r^s = 0.08\, m^3\, min^{-1}$	$h_2 = 2.2 \cdot 10^4\, kJ\, kmol^{-1}$
$c_B^s = 1.1975\, kmol\, m^{-3}$	$q_c^s = 0.08\, m^3\, min^{-1}$

The input and output signals further used for control purposes are defined by

$$u(t) = q_c(t) - q_c^s, y(t) = T_r(t) - T_r^s \qquad (60)$$

Steady-states of the CSTR

The steady-states of the reactor and corresponding static characteristic was obtained as the dependence of steady-state outputs on inputs with the help of the presented simulation model. The static characteristics will then be inverted, approximated, and used in the SNP part of the Wiener model, as well as for the limit point values calculated in the following text.

At the operating point $q_c^s = 0.08\, m^3\, min^{-1}$, $T_r^s = 324.80\, K$, boundary values of the operating interval were chosen as q_{cmin}, q_{cmax} and limit points q_{cL}, q_{cU}:

$$q_{cmin} = 0.02\, m^3\, min^{-1} \qquad q_{cL} = 0.016\, m^3\, min^{-1}$$

$$q_{cmax} = 0.12\, m^3\, min^{-1} \qquad q_{cU} = 0.13\, m^3\, min^{-1}$$

Control of the CSTR Using the Wiener Model

The controller was designed according to Section 4.1. This part provides the final relations together with schematic representations and the results achieved.

Static Nonlinear Part

Static-characteristic values were processed according to (15), where $\eta = T_r$ and $\upsilon = q_c$.

The resulting function $\psi = f(\gamma)$ was inverted and approximated by an exponential function:

$$\gamma = -74071.7 + 2.4589 \exp\left(-\frac{\psi}{3.967}\right) + 74076 \exp\left(-\frac{\psi}{697475}\right) \qquad (61)$$

The derivative needed for computing $u(t)$ (16) is

$$\frac{d\gamma}{d\psi} = -0.6198 \exp\left(-\frac{\psi}{3.967}\right) - 0.1062 \exp\left(-\frac{\psi}{697475}\right) \qquad (62)$$

External Linear Model

The analysis is based on simulated step responses of the SNP+CSTR system near the operating point $q_c^s = 0{,}08\, m^3\, min^{-1}$, $T_r^s = 324{,}80\, K$.

Based on the results obtained, a second-order model of the system was selected:

$$\ddot{y}(t) + a_1\dot{y}(t) + a_0 y(t) = b_0 u_0(t) \qquad (63)$$

with the transfer function (18) as:

$$G(s) = \frac{Y(s)}{U_0(s)} = \frac{b_0}{s^2 + a_1 s + a_0} \qquad (64)$$

Parameter Estimation

Filter parameters in (21), (22) were selected as

$$c(s) = s^2 + c_1 s + c_0 = s^2 + 1.5s + 0.5 \qquad (65)$$

to provide suitable dynamical properties enabling capturing the main dynamics of the given process to be identified and controlled. For the second-order model, the regressor vector is

$$\boldsymbol{\phi}(t_k) = \left[-y_f(t_k) - y_f^{(1)}(t_k)\; u_{0f}(t_k)\; 1\right] \qquad (66)$$

The parameter vector

$$\boldsymbol{\Theta}^T(t_k) = [a_0\; a_1\; b_0\; \mu] \qquad (67)$$

is obtained by solving (25).

Dynamic Linear Part

The structure of the Q and R regulators (28) is based on the structure of the controlled system, represented by the transfer function (64). For the polynomial degree $a(s)$, $\deg a = 2$, the degrees of the unknown polynomials are

$$\deg q = 2, \deg \tilde{p} = 1, \deg r = 0, \deg d = 4 \qquad (68)$$

The transfer functions of the regulators are therefore

$$Q(s) = \frac{q(s)}{s\tilde{p}(s)} = \frac{q_2 s^2 + q_1 s + q_0}{s(s + p_0)} \qquad (69)$$

$$R(s) = \frac{r(s)}{s\tilde{p}(s)} = \frac{r_0}{s(s + p_0)} \qquad (70)$$

and the characteristic polynomial $d(s)$ is of the form:

$$d(s) = n(s)(s+\alpha)^2, \qquad (71)$$

where

$$n(s) = s^2 + n_1 s + n_0,\ n_0 = \sqrt{a_0^2},\ n_1 = \sqrt{a_1^2 + 2n_0 - 2a_0} \qquad (72)$$

and α > 0 is a further tuning parameter. The matrix equation (73), which is the result of solving the polynomial equations (31) by the method of undetermined coefficients, allows obtaining the parameters of the regulators (69), (70).

$$\begin{pmatrix} 1 & 0 & 0 & 0 \\ a_1 & b_0 & 0 & 0 \\ a_0 & 0 & b_0 & 0 \\ 0 & 0 & 0 & b_0 \end{pmatrix} \begin{pmatrix} \tilde{p}_0 \\ q_2 \\ q_1 \\ q_0 \end{pmatrix} = \begin{pmatrix} d_3 - a_1 \\ d_2 - a_0 \\ d_1 \\ d_0 \end{pmatrix}, \qquad (73)$$

with

$$d_3 = n_1 + 2\alpha, d_2 = 2\alpha n_1 + n_0 + \alpha^2, \quad d_1 = 2\alpha n_0 + \alpha^2 n_1, d_0 = \alpha^2 n_0 \qquad (74)$$

Simulation of CSTR Control with the Wiener Model

A graphical representation of the entire adaptive control system is shown in Figure 13.

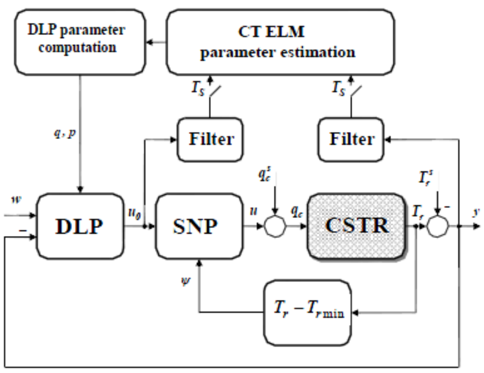

Figure 13. Control system with the Wiener model [1]

Before the actual control of the system, the initial settings of the DLP regulators must be obtained. For this purpose, an adaptation phase is used, which first identifies the SNP+CSTR system in the control loop with a simple proportional controller (see Figure 14 below). Based on the identified model parameters, the initial parameters of the Q and R regulators are calculated; during the actual control, these parameters are re-computed at each simulation step.

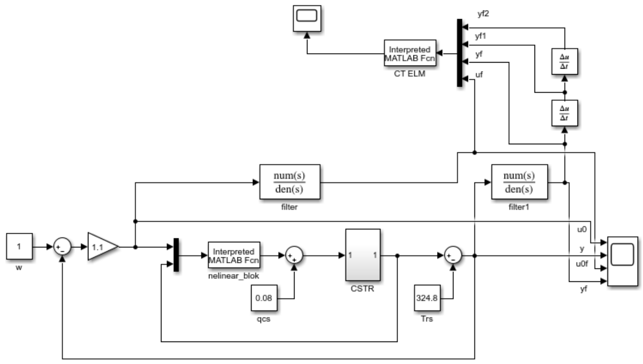

Figure 14. Simulink diagram for the adaptation phase

The SNP+CSTR system model was identified in the adaptation phase as

$$G(s) = \frac{Y(s)}{U_0(s)} = \frac{b_0}{s^2 + a_1 s + a_0} = \frac{0{,}0046}{s^2 + 0.1458s + 0.0039} \qquad (75)$$

The control simulation was also implemented in Matlab/Simulink environment; the simulation scheme (Figure 15) and the results of the control process (Figure 16) are shown below.

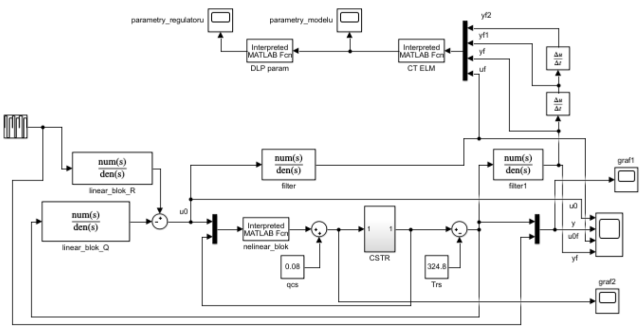

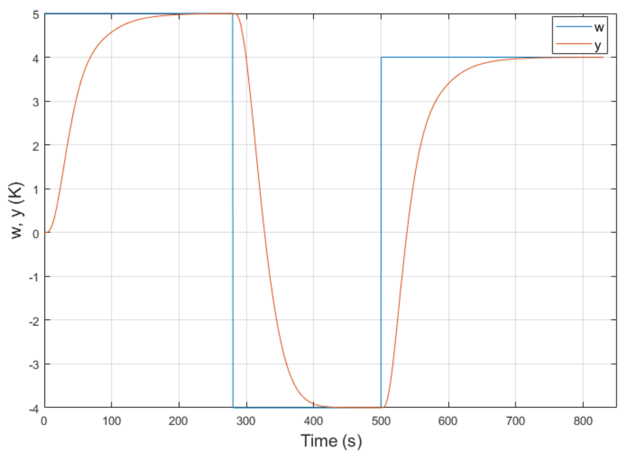

Figure 15. Control response of reactor temperature deviation

5.3. Comparison of Sequential Linearization and Wiener-Model Control

To compare the proposed linear and nonlinear control approaches, two methods applied to the SISO tank system were selected: sequential linearization (with $\alpha = 0.2$) and the Wiener-model-based method (with $\alpha = 0.3$). The results of the control are shown below in Figure 17:

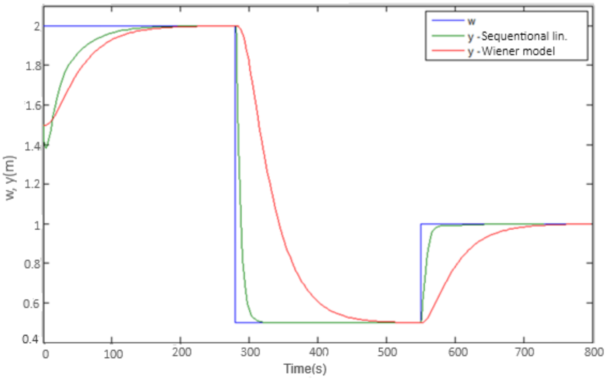

Figure 17. Comparison of polynomial approach with sequential linearized model and control with Wiener model [1].

The graph demonstrates that the approach combining sequential linearization and subsequent polynomial control provides superior performance, especially in terms of reference tracking and corresponding settling times.

Conclusion

In this work, two possible control strategies for nonlinear systems were analysed and compared together in detail. The first strategy was based on sequential linearization combined with polynomial approach, while the second employed a Wiener model. The study demonstrated that the sequential linearization with suitably implemented polynomial approach provided consistently better performance than the Wiener model. The presented results confirm the suitability of the proposed approach for improving control performance when dealing with nonlinear processes. Moreover, the findings indicate that this method can serve as a promising foundation for further research and potential applications in other similar control tasks. Possible limitations of the presented approach can stem from the fact that all the calculations must be done in real-time within a given sampling period, however, since the current control is carried out entirely in simulation, the computational load is very low (with execution time around 1.2 seconds in MATLAB/Simulink). If the control were implemented on a real system, for example on a microcontroller, the computational load would certainly be significantly higher. Nevertheless, taking into account possibilities of nowadays hardware and software tools and relatively slow dynamics of industrial processes this does not seem too restrictive.

Future plans include continuing with the combination of sequential linearization and the 1DOF polynomial control approach and exploring the integration of AI into the polynomial control component.

Acknowledgements.
This research was funded by the Internal Grant Agency of Tomas Bata University supported under project No. IGA/CebiaTech/2024/002.

References

[1] Kurečková, E. Vybrané metody nelineárního řízení [in czech]. Master thesis. Supervisor prof. Ing. Petr Dostál, CSc. Zlin: Tomas Bata University in Zlin; 2013.
[2] Astolfi, A., Karagiannis, D., Ortega, R. Nonlinear and Adaptive Control with Applications, London: Springer-Verlag; 2008.
[3] Gavendová, E., Vojtěšek, J. Review of Modern Nonlinear Control Methods. Innovations in Mechatronics Engineering IV. In Proceedings of International Conference Innovation in Engineering 2025. June 18-20; Prague. Springer Nature Switzerland; 2025, p. 265-274.
[4] Dostál, P., Bakošová, M., Vojtěšek, J., Bobál, V. Chemical Papers 65 (5); 2011, Adaptive nonlinear control of a continuous stirred tank reactor; p. 635-643.
[5] Čelikovský, S. Nelineární systémy [in czech]. Prague: CTU in Prague; 2006.
[6] Iqbal, J., Ullah, M., Khan, S., Khelifa, B., Ćuković, S. Nonlinear control systems – A brief overview of historical and recent advances. Nonlinear Engineering 2017 6(4), 2017, p. 301-312.
[7] Abdelwahed, I., Bouzrara, K. Nonlinear Model Predictive Control Based on Second-Order NARX-Laguerre Model for Twin Rotor System Control, Iranian Journal of Science and Technology; 2024.
[8] Öztekin, M., Kiselychnyk, O., Wang, J. Nonlinear Optimal Control for Interior Permanent Magnet Synchronous Motor Drives, European Control Conference, London; 2020.
[9] Gardi, A., Sabatini, R., Kistan, T. Multi-Objective Trajectory Optimisation Algorithms for Avionics and ATM Systems, Sustainable Aviation Technology and Operations: Research and Innovation Perspectives, 2024, p. 433-457.
[10] Bali, A., Singh, U., Kumar, R., Jain, S. Neural Networks Based-Adaptive Control of Non-linear Ship Manoeuvring System, Journal of Control, Automation and Electrical Systems 2024, 2024, p. 314-325.
[11] Maaruf, M., Ali, M., Al-Sunni, F. Artificial intelligence-based control of continuous polymerization reactor with input dead-zone, International Journal of Dynamics and Control 2023, 2023. p. 1153–1165.
[12] De Persis, C., Rotulo, M., Tesi, P. Learning controllers from data via approximate nonlinearity cancellation, IEEE Transactions Automatic Control, 2023; p. 1–16.
[13] Dai, X., De Persis, C., Monshizadeh, N., Tesi, P. Data-driven control of nonlinear systems from input-output data, Proceedings of the 62nd IEEE Conference on Decision and Control, Singapore; 2023.
[14] Dostál, P., Vojtěšek, J., Bobál. Simulation of the 2DOF nonlinear adaptive control of a chemical reactor. In:

Proceeding of 25th European Conference on Modelling and Simulation. June 7-10; Krakow, Poland; 2011, p. 494-499.
[15] Ahlén, A., Casavola, A., Grimble, M., Hunt, K., Ježek, J., Kučera V., Loiseau, J., Mosca, E., Šebek, M., Sternad, M., Zagalak, P. Polynomial methods in optimal control and filtering, London: Peter Peregrinus Ltd.; 1993